Inorganic Chemistry

Article

pubs.acs.org/IC

Role of the Coordination Center in Photocurrent Behavior of a Tetrathiafulvalene and Metal Complex Dyad

Yong-Gang Sun,[†] Shu-Fang Ji,[†] Peng Huo,[†] Jing-Xue Yin,[†] Yu-De Huang,[†] Qin-Yu Zhu,*[,†,‡] and Jie Dai*[,†,‡]

[†]College of Chemistry, Chemical Engineering and Materials Science, Soochow University, Suzhou 215123, P. R. China

[‡]State Key Laboratory of Coordination Chemistry, Nanjing University, Nanjing 210093, P. R. China

Supporting Information

ABSTRACT: Small organic molecule-based compounds are considered to be promising materials in photoelectronics and high-performance optoelectronic devices. However, photoelectron conversion research based on functional organic molecule and metal complex dyads is very scarce. We design and prepare a series of compounds containing a tetrathiafulvalene (TTF) moiety substituted with pyridylmethylamide groups of formulas $[Ni(acac)_2L]\cdot 2CH_3OH$ (**1**), $[Cu_2I_2L_2]\cdot THF\cdot 2CH_3CN$ (**2**), and $[MnCl_2L_2]_n\cdot 2nCH_3CH_2OH$ (**3**) (L = 4,5-bis(3-pyridylmethylamide)-4′,5′-bimethylthio-tetrathiafulvalene, acac = acetylacetone) to study the role of the coordination center in photocurrent behavior. Complex **1** is a mononuclear species, and complex **2** is a dimeric species. Complex **3** is a two-dimensional (2-D) coordination polymer. Spectroscopic and electrochemical properties of these complexes indicate that they are electrochemically active materials. The tetrathiafulvalene ligand L is a photoelectron donor in the presence of electron acceptor methylviologen. The effect of metal coordination centers on photocurrent response behavior is examined. The redox-active metal coordination centers should play an important role in improvement of the photocurrent response property. The different morphologies of the electrode films reflect the dimensions in molecular structures of the coordination compounds.

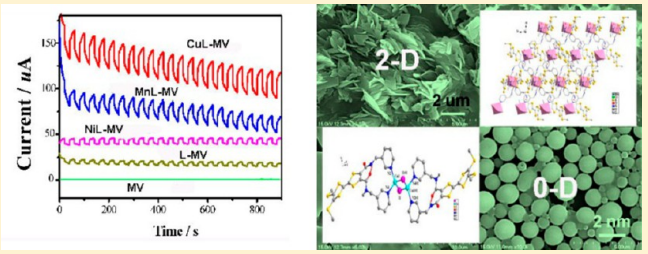

INTRODUCTION

The research of molecule-based materials for organic electronics is one of the current challenges in photoelectronic material science due to their advantages of easy fabrication, simple device structure, low cost, light weight, and capability to be fabricated into flexible devices.[1] Various small molecular classes, including fullerene-, phthalocyanine-, oligothiophene-, and acene-based derivative, are commonly used for application in optoelectronic devices and solar cells.[2] Tetrathiafulvalene (TTF) is a prominent redox-active molecule for its two-step reversible one-electron redox processes and also a good electron donor attributed to its sulfur-rich structure. Recently, molecule dyads or triads with a TTF moiety have received considerable interest because combination of the TTF moiety with several kinds of organic electron acceptors has expanded the possibility for novel photoelectron conversion materials.[3−6] The photoinduced intra- or intermolecular charge-transfer interactions between the electron donor and acceptor parts and resultant formation of the charge-separated state have played an important role for development of optoelectronic devices. For example, a donor−acceptor TTF−BODIPY dyad was synthesized to develop new photoconducting materials;[3b] a TTF−P−C_{60} triad displayed photovoltaic property to realize high solar energy conversion efficiency.[6b]

The design and synthesis of the TTF derivatives functionalized by various mono- or polydentate coordination groups along with the corresponding metal complexes have been extensively carried out during the past decade.[7,8] The strategies are based on the varieties of the transition metal complexes in their chemophysical properties, such as electron transit property, photoactivity, and redox property. The synergistic effect of metal complexes with the TTF moiety in the dyad or multicomponent systems will be a promising property for functional materials. For example, some TTF−metal coordination dyads with TTF−pyridyl ligands and transition metals or lanthanide metals coordination centers have been recently synthesized and structurally characterized.[8−13] The properties that research is mainly concerned with are the semiconductivity and magnetic susceptibility of these transition metal compounds. Partial oxidation of the TTF moiety and the pyridyl-coordinated transition metal group yielded the paramagnetic or conductive π−d complexes.[9c,10c] Photophysical measurements reveal that the tetrathiafulvalene moiety is a versatile antenna for lanthanide infrared luminescence upon excitation in the charge transfer band.[9a] However, research on the photoelectron conversion properties based on such metal coordination TTF dyads is very scarce. Our research interest is concentrated on the photocurrent response properties of the TTF metal coordination system and the effect of the metal coordination centers on the photoactive properties.

Received: December 4, 2013
Published: March 4, 2014

   dx.doi.org/10.1021/ic402993y | *Inorg. Chem.* 2014, 53, 3078−3087

In this work, we use a flexible bifunctional TTF ligand, 4,5-bis(3-pyridylmethylamide)-4′,5′-bimethylthio-tetrathiafulvalene (TTF−$(CONHCH_2\text{-}Py)_2$, **L**) (Chart 1), in which the pyridyl group is combined with the TTF moiety through an amide−methylene bridge. The TTF−pyridyl derivative is selected because of the good coordination ability of the pyridyl group. The flexible ligand is designed because such ligand can adopt various conformations according to the restrictions imposed by the coordination requirement of the metal. The role of the metal coordination center in photoelectric conversion behavior is studied based on the TTF−py compound L and three transition metal complexes, $[Ni(acac)_2L]\cdot 2CH_3OH$ (**1**), $[Cu_2I_2L_2]\cdot THF\cdot 2CH_3CN$ (**2**), and $[MnCl_2L_2]_n\cdot 2nCH_3CH_2OH$ (**3**) (acac = acetylacetone). All three compounds have been characterized by single-crystal X-ray diffraction. The photocurrent properties are studied using microcrystal electrodes and wet-coated film electrodes. The different film morphologies of the electrodes and photocurrent behaviors are discussed in the viewpoint of molecular structures.

Chart 1. Structure of the Ligand DMT−TTF−$(CONHCH_2\text{-}Py)_2$

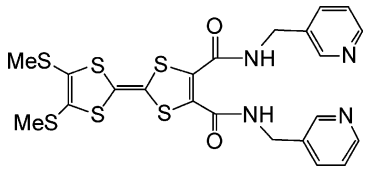

EXPERIMENTAL SECTION

General Remarks. All reagents for syntheses and analyses were of analytical grade. Elemental analyses of C, H, and N were performed using an EA1110 elemental analyzer. IR spectra were recorded as KBr pellets on a Nicolet Magna 550 FT-IR spectrometer. Electronic absorption spectra were measured on a Shimadzu UV-3150 spectrometer. Cyclic voltammetry (CV) of the solid-state compounds was investigated on a CHI600 electrochemistry workstation in a three-electrode system using a crystal-coated ITO glass as a working electrode, a Pt wire auxiliary electrode, and a saturated calomel electrode (SCE) as the reference. The morphologies of the films were observed with a JSM-5600LV scanning electron microscope (SEM). Energy-dispersive spectroscopy (EDS) was collected on a D/MAX-3C diffractometer using a Cu tube source (Cu Kα, λ = 1.5406 Å).

Preparation of Compounds. *DMT-TTF-$(CONHCH_2\text{-}Py)_2$ (**L**).* The ligand 4,5-bis(3-pyridylmethylamide)-4′,5′-bimethylthiotetrathiafulvalene, DMT−TTF−$(CONHCH_2\text{-}Py)_2$ (**L**) was synthesized using a modified method according to the literature.[14] A CH_3CN (25 mL) solution of $(CH_3S)_2TTF(COOMe)_2$ (400 mg, 0.96 mmol) was reacted with an excess of 3-aminopyridine in aqueous solution (50% w/w). After 24 h of stirring at room temperature, the resulting precipitate was filtered and recrystallized twice from tetrahydrofuran (THF). Purple powder was obtained (0.45g, 83%). Anal. Calcd for $C_{22}H_{20}N_4O_2S_6$: C, 46.79; H, 3.56; N, 9.92. Found: C, 46.40; H, 3.55; N, 9.93. IR (KBr, cm^{-1}): 3427, 3296, 3064, 3025, 2933, 1643, 1574, 1481, 1427, 1382, 1034, 787.

*$[Ni(acac)_2L]\cdot 2CH_3OH$ (**1**).* $Ni(acac)_2$ (20 mg, 0.02 mmol) in methanol (1 mL) and cyclohexane (10 mL) was dropwise added to **L** (22 mg, 0.04 mmol) in methanol (20 mL) and dichloromethane (2 mL). The mixture was stirred for 1 h at room temperature and filtered into a beaker; then red block single crystals of **1** were obtained in 5 days from the filtrate by controlled evaporation of the solvent and used for all measurements (5.6 mg, yield 31.6%). Anal. Calcd for $C_{34}H_{42}N_4Ni\ O_8S_6$: C, 46.10; H, 4.78; N, 6.33. Found: C, 45.66; H, 4.19; N, 6.56. IR data (cm^{-1}): 3319, 3064, 2925, 1659, 1560, 1421, 1282, 1019, 764 cm^{-1}.

*$[Cu_2I_2L_2]\cdot THF\cdot 2CH_3CN$ (**2**).* CuI (1.9 mg, 0.01 mmol) in acetonitrile (2 mL) was dropwise added to **L** (11.2 mg, 0.02 mmol) in tetrahydrofuran (THF) (3 mL). The mixture was stirred for 30 min at room temperature and filtered into a glass tube; dark red block single crystals of **2** were obtained in 7 days from the filtrate by controlled evaporation of the solvent and used for all measurements (5.0 mg, yield 30.2%). Anal. Calcd for $C_{52}H_{54}Cu_2I_2N_{10}O_5S_{12}$: C, 37.52; H, 3.27; N, 8.41. Found: C, 37.19; H, 3.22; N, 8.18. IR data (cm^{-1}): 3427, 3296, 3026, 2933, 1643, 1567, 1481, 1427, 1382, 787 cm^{-1}.

*$[MnCl_2L_2]_n\cdot 2nCH_3CH_2OH$ (**3**).* Single crystals of **3** were obtained by H-shaped glass tube diffusion. The dichloromethane solution (8 mL) of

Table 1. Crystal Data and Structural Refinement Parameters for 1−3

	1	2	3
formula	$C_{34}H_{42}N_4NiO_8S_6$	$C_{52}H_{54}Cu_2I_2N_{10}O_5S_{12}$	$C_{48}H_{52}Cl_2MnN_8O_6S_{12}$
fw	885.79	1664.65	1347.55
cryst size (mm^3)	0.32 × 0.30 × 0.09	0.62 × 0.60 × 0.20	0.43 × 0.30 × 0.10
cryst syst	monoclinic	triclinic	monoclinic
space group	*P*2/*n*	*P*-1	$P2_1/n$
a (Å)	8.7233(8)	9.4978(13)	17.167(3)
b (Å)	9.9107(9)	13.3237(19)	8.5626(11)
c (Å)	47.563(5)	14.205(2)	19.717(3)
α (deg)	90.00	77.790(10)	90.00
β (deg)	91.594(3)	76.450(9)	93.173(4)
γ (deg)	90.00	73.682(9)	90.00
V ($Å^3$)	4110.5(7)	1656.6(4)	2893.8(7)
Z	4	1	2
ρ_{calcd} (g cm^{-3})	1.431	1.669	1.546
F(000)	1848	832	1390
μ (mm^{-1})	0.829	2.004	0.808
T (K)	223(2)	223(2)	223(2)
no. of reflns collected	9160	6768	10 033
no. of unique reflns	6997	6015	5285
no. of obsd reflns	5083	5577	4657
no. params	486	376	345
GOF on F^2	1.046	1.086	1.163
R_1 [$I > 2\sigma(I)$]	0.0899	0.0312	0.0596
wR_2 [$I > 2\sigma(I)$]	0.1436	0.0717	0.1458

dx.doi.org/10.1021/ic402993y | Inorg. Chem. 2014, 53, 3078−3087

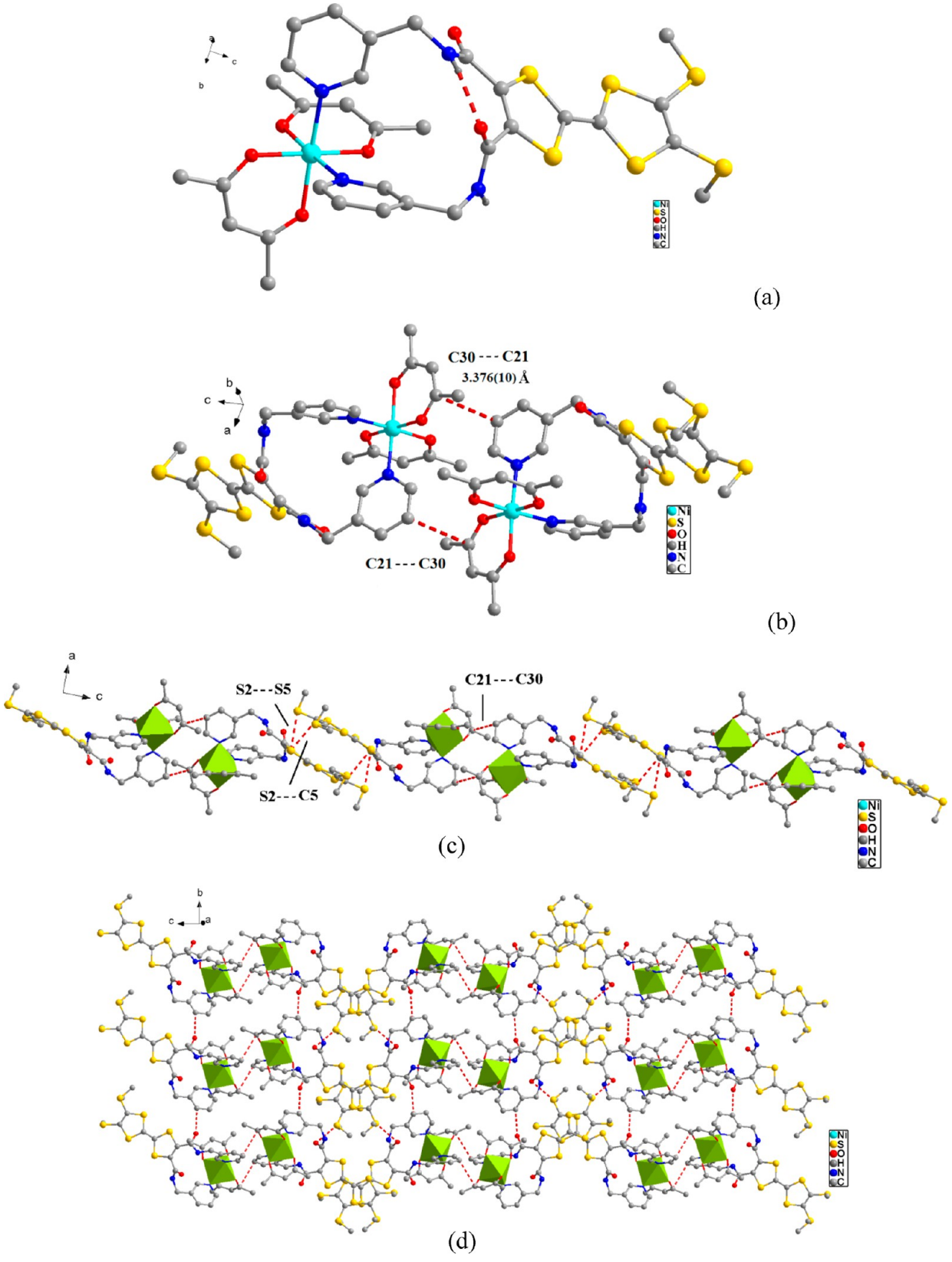

Figure 1. (a) Molecular structure of **1**; (b) view of the dimer structure showing the C21···C30 short contacts between two molecules; (c) view of the chain structure; (d) view of the two-dimensional network, illustrating the interchain short contacts. Uncoordinated solvent molecules and hydrogen atoms were omitted for clarity.

L (44.6 mg, 0.04 mmol) was added to one side of an H tube, and the saturated ethanol solution (5 mL) of $MnCl_2·4H_2O$ was added to the other side of the H tube. The two sides were connected by additional ethanol and left in the dark at room temperature. Red single crystals **3** were obtained on the bottom of the tube after a month (7.8 mg, yield 28.9% based on L). Anal. Calcd for $C_{48}H_{52}Cl_2MnN_8O_6S_{12}$: C, 42.78; H,

dx.doi.org/10.1021/ic402993y | *Inorg. Chem.* 2014, 53, 3078−3087

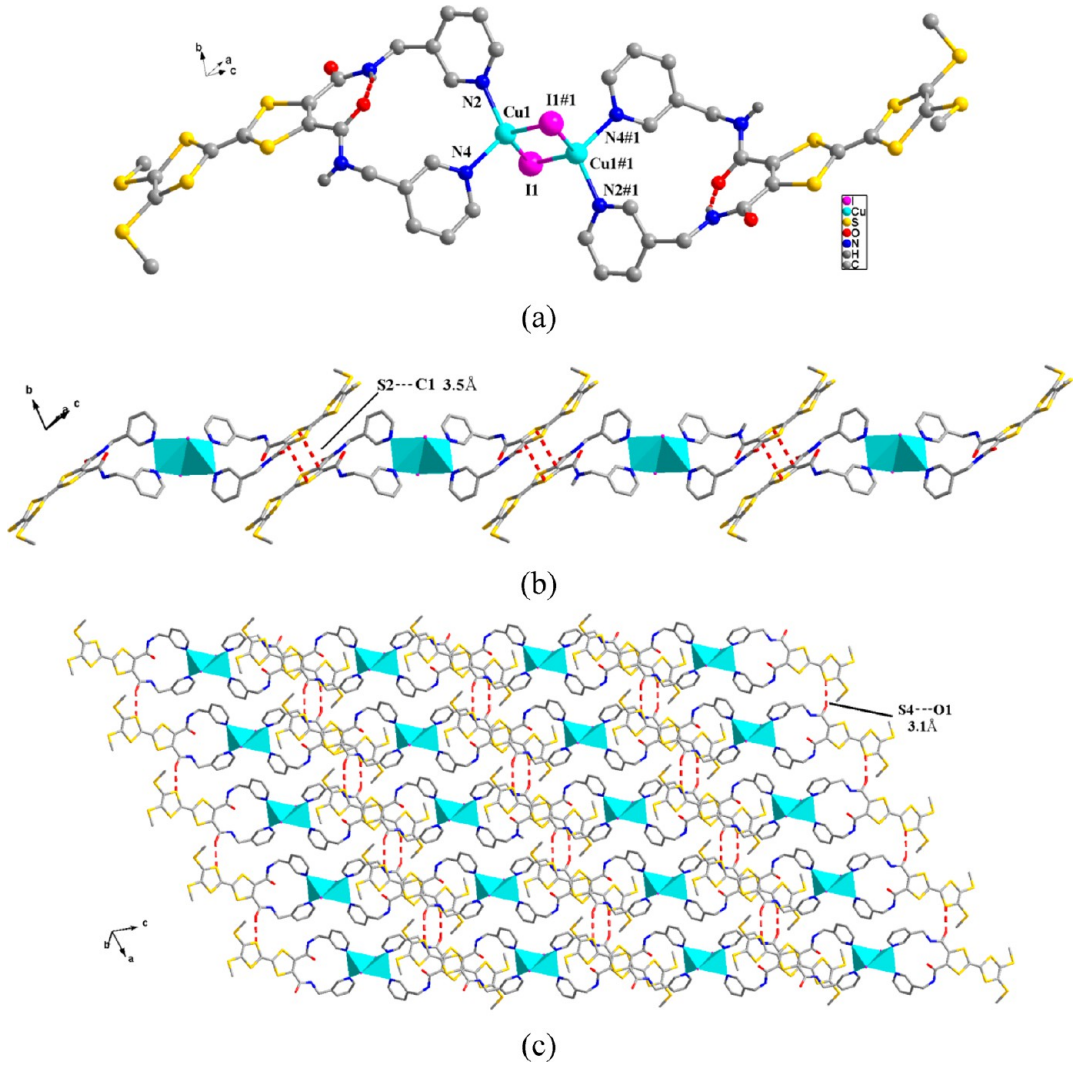

Figure 2. (a) Dimeric structure of **2**; (b) view of the chain structure, illustrating the intermolecular C1···S2 short contacts; (c) view of the two-dimensional network, illustrating the interchain O1···S4 short contacts. Uncoordinated solvent molecules and hydrogen atoms were omitted for clarity.

3.89; N, 8.32. Found: C, 42.40; H, 3.79; N, 7.90. IR data (cm^{-1}): 3267, 1636, 1559, 1428, 1358, 1049, 888 cm^{-1}.

X-ray Crystallographic Study. The measurement was carried out on a Rigaku Mercury CCD diffractometer at low temperature with graphite-monochromated Mo Kα (λ = 0.71073 Å) radiation. X-ray crystallographic data were collected and processed using CrystalClear (Rigaku).[15] The structure was solved by direct methods using SHELXS-97, and refinement against all reflections of the compound was performed using SHELXL-97.[16] All non-hydrogen atoms were refined anisotropically. Hydrogen atoms were positioned with idealized geometry and refined with fixed isotropic displacement parameters. Relevant crystal data, collection parameters, and refinement results can be found in Table 1. Selected bond lengths for compounds **1**−**3** are listed in Table SI1 (Supporting Information).

Preparation of the Films. Films were prepared by wet solution methods, including the direct solution coating method and the layer-by-layer reaction method. The direct solution coating method is simply dissolving the compounds (0.01 mmol) in 3 mL of THF solvent or the mixed solvents of THF−MeOH for **1** and CH_3CN−THF for **2**. The resulting solutions were coated on a glass, and then the solvents were removed by evaporation to yield the respective films. The layer-by-layer reaction method is dissolving the ligand L (0.01 or 0.02 mmol) and the metal precursor compounds (0.01 or 0.02 mmol) in 3 mL of mixed solvents of $CHCl_3$−MeOH, THF−THF for **1**, $CHCl_3$−CH_3CN for **2**, and THF−THF, THF−MeOH, $CHCl_3$−MeOH, and CH_2Cl_2−MeOH for **3**, respectively. All ratios of the mixed solvents are 1:1 by volume. The L solution was first coated on a glass and evaporated, and then a solution of the metal compound was coated on the L layer. The as-prepared films of **1**−**3** were checked by FTIR (Figure SI1, Supporting Information).

Preparation of the Photoelectrodes. Photoelectrodes of the microcrystals (denoted as ML/ITO) were prepared by the powder coating method. Crystals of compounds were grinded and pressed uniformly on the ITO glass (100 Ω/□). Preparation of the electrodes used in the solid-state CV measurement is the same. Photoelectrodes of the films (denoted as M−L/ITO) were prepared by the same method as those of the preparation of the films except that the glass is replaced by the ITO glass. The film area is 1.0 × 1.0 cm^2.

Photocurrent Measurement. Photocurrent experiments were performed on a CHI650E electrochemistry workstation in a three-electrode system, ML/ITO or M−L/ITO as the working electrode with an effective irradiation area of 1.0 cm^2, Pt wire as an auxiliary electrode, and a saturated calomel electrode (SCE) as the reference electrode. The supporting electrolyte solution was 0.1 mol·L^{-1} sodium sulfate aqueous solution. A 150 W high-pressure xenon lamp, located 20 cm away from the surface of the ITO electrode, was employed as a light source. All photocurrent measurements were carried out under the same experimental condition. The lamp was kept on continuously, and a manual shutter was used to block exposure of the sample to the light. The sample was typically irradiated over 0−900 s with an interval 20 s.

dx.doi.org/10.1021/ic402993y | Inorg. Chem. 2014, 53, 3078−3087

RESULTS AND DISCUSSION

Structure Discussion. *[Ni(acac)$_2$L]·2CH$_3$OH (**1**).* Mixing a methanol and cyclohexane (1:10 by volume) solution of Ni(acac)$_2$ with a methanol and dichloromethane (10:1 by volume) solution of **L** gave crystals **1** suitable for X-ray analysis. As shown in Figure 1a, **1** is a mononuclear complex crystallized in the monoclinic $P2/n$ space group, and the asymmetric unit consists of one nickel atom, one ligand L, two acac anions, and two cocrystallized methanol molecules. The Ni(II) ion is six coordinated by two chelating N atoms from the pyridine arms of one L and four oxygen atoms from two acac anions, thereby forming a slightly distorted octahedral coordination geometry. The NiO and NiN bond lengths in this compound are the same as those in Ni(acac)$_2$(Py-TTF)$_2$.[9d]

Two molecules are linked by C21···C30 (3.376(10) Å) short contacts to form a dimer (Figure 1b), which is further connected by S2···S5 (3.427(3) Å) and S2···C5 (3.477(9) Å) short contacts to form a one-dimensional chain (Figure 1c). Each chain is assembled through O1···S6 (3.314(6) Å) and O2···C15 (3.055(9) Å) short contacts leading to formation of an overall two-dimensional network (Figure 1d).

*[Cu$_2$I$_2$L$_2$]·THF·CH$_3$CN (**2**).* Mixing an acetonitrile solution of CuI with a tetrahydrofuran solution of **L** (2:3 by volume) gave crystals **2** suitable for X-ray analysis. Complex **2** is a dimetallacyclic species crystallized in the triclinic space group $P\bar{1}$. As shown in Figure 2a, the dimer is formed from two L ligands, joined together by the Cu2I2 core, related by a center of symmetry at the midpoint between the two Cu(I) atoms. The asymmetric unit contains one copper atom, one L ligand, one iodide ion, one-half tetrahydrofuran, and one-half acetonitrile solvent molecules. The Cu(I) ion shows a distorted tetrahedral coordination geometry by two bridging iodide atoms and two chelating N atoms from the pyridine arms of one L. The Cu−I distances are in the range of 2.6392(10)−2.6473(6) Å, and Cu−N distances are 2.056(2)−2.062(2) Å, as comparable to those reported in dimer Cu2I2N2 species.[17] The Cu−Cu distance (2.6296(8) Å) is at the beginning of the range for other complexes with Cu2I2 cores (2.566−3.452 Å).[18] The Cu2I2 core is strictly planar, and the py rings of the ligand L are almost coplanar with mean deviations of 0.0079(29) and 0.0027(27) Å, respectively. The dihedral angle between the two five-membered rings of the TTF core is 21.208(69)°.

A one-dimensional polymeric chain, which propagated along the [1-11] diagonal axis, is formed through C1···S2 (3.495(3) Å) short contacts (Figure 2b). Each chain is further assembled through O1···S4 (3.093(2) Å) short contacts, leading to formation of an overall two-dimensional network (Figure 2c).

*[MnCl$_2$L$_2$]$_n$·2nCH$_3$CH$_2$OH (**3**).* A new strategy was adopted for coordination of the ligand L on Mn(II) centers. H-shaped glass tube slow diffusion of solutions of the ligand and of MnCl$_2$·4H$_2$O (8:5 by volume) afforded crystals of complex **3**, for which structural analysis revealed the first two-dimensional (2-D) manganese coordination polymer based on TTF−amide−py. Complex **3** crystallizes in the monoclinic $P2_1/n$ space group, and the asymmetric unit consists of one-half manganese atom, one ligand L, one chlorine atom, and one cocrystallized methanol molecule. The structure is depicted in Figure 3a (#1 $-x, 2-y, 1-z$; #2 $-0.5+x, 1.5-y, 0.5+z$; #3 $0.5-x, 0.5+y, 0.5-z$). The Mn(II) ion resides at the inversion center of a 4 + 2 square-elongated octahedron, with Mn1−N2, Mn1−N4, and Mn1−Cl1 bond distances of 2.339(4), 2.305(4), and 2.486(1) Å, respectively. Bond angles within the coordination sphere deviate appreciably from the expected 90° angles which range from 85.60(13)° to 94.40(13)°. The Mn atom and four N atoms

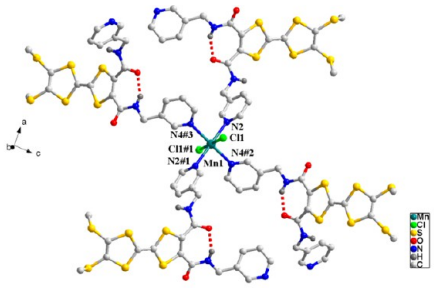

(a) (#1: -x, 2-y, 1-z; #2: -0.5+x, 1.5-y, 0.5+z; #3: 0.5-x, 0.5+y, 0.5-z)

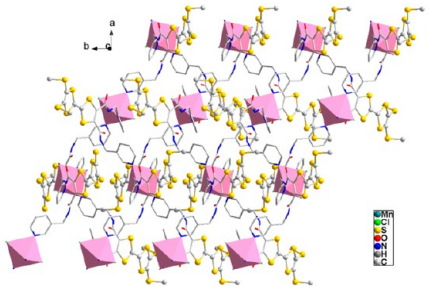

(b)

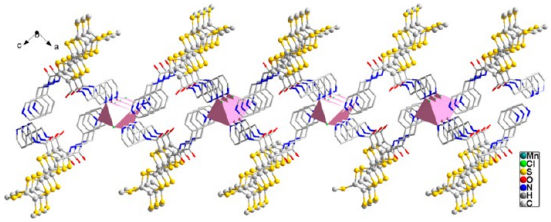

(c)

Figure 3. (a) Coordination environment of Mn(II) in **3**; (b) 2-D network constructed by the L ligands along the *bc* plane (TTF moieties are omitted for clarity); (c) 2-D network constructed by the L ligands along the *ac* plane. Uncoordinated ethanol molecules in a−c and hydrogen atoms except those of amido groups in a were omitted for clarity.

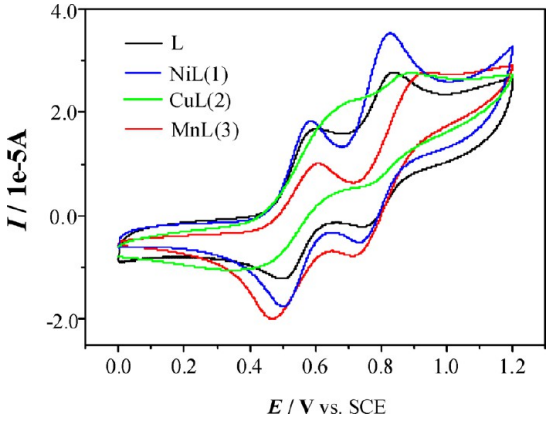

Figure 4. Cyclic voltammogram of the solid-state compounds of L and **1**−**3** in CH$_3$CN (0.1 mol·L^{-1} Bu$_4$NClO$_4$, 100 mV s^{-1}).

dx.doi.org/10.1021/ic402993y | Inorg. Chem. 2014, 53, 3078−3087

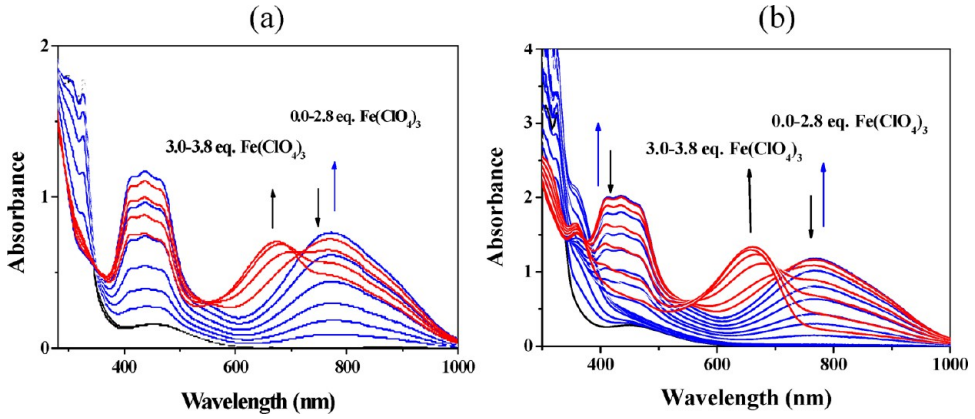

Figure 5. Absorption spectra of L (a) and **1** (b) (1.0×10^{-4} mol·L^{-1}) in CH_2Cl_2−CH_3CN (1:1 by volume) in the presence of increasing quantities of $Fe(ClO_4)_3 \cdot 6H_2O$.

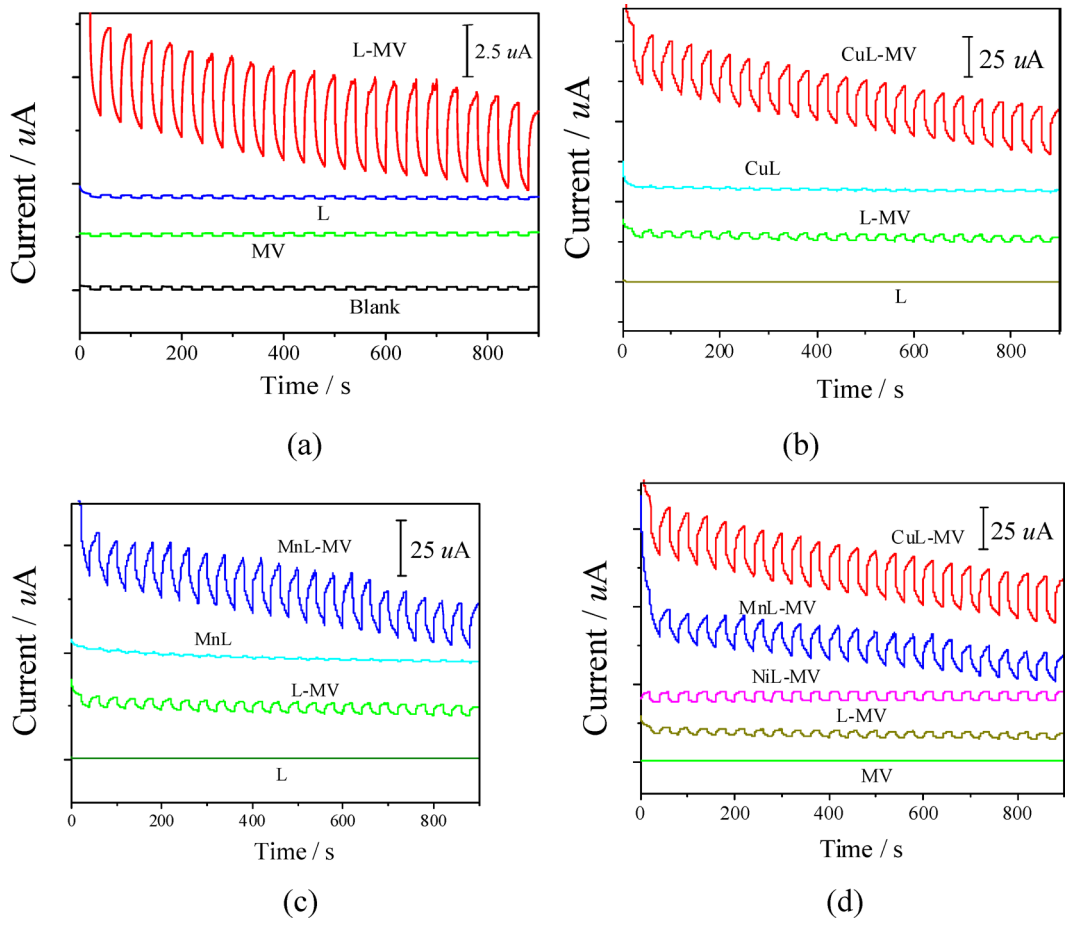

Figure 6. Photocurrent responses of (a) L-modified electrode along with the comparative electrodes (blank test (black line), MVI_2 (green line), L (blue line), and L−MV (red line)); (b) microcrystal CuL-modified electrodes along with the comparative electrodes (L (olive line), L-MV (green line), CuL complex (cyan line), and CuL−MV (red line)); (c) L (olive line), L−MV (green line), MnL complex (cyan line), and MnL−MV (blue line); (d) MV (green line), L−MV (olive line), NiL−MV (magenta line), MnL−MV (blue line), and CuL−MV (red line). Three-electrode system, 0.10 mol·L^{-1} aqueous solution of Na_2SO_4. Lines are separated to be of clarity, and the *Y* axis only shows the relative current intensity.

resided in a MnN4 strict plane. The py rings of the ligand L are also almost coplanar with mean deviations of 0.0014(1) and 0.0083(0) Å, respectively. The angles between the MnN4 plane and the pyridine rings are 69.9° and 50.1°. The dihedral angle between the two five-membered rings of the TTF core is 19.8°. Each L bridges two Mn1 centers, and thus, each CuN4Cl2 octahedron connects with four other octahedra (Figure 3b) to form a 2D network structure parallel to the (101) plane (Figure 3b and 3c). The S5···O1 (3.257 Å) and S···Cl (3.306 Å) short contacts link the 2D network to form a 3D supramolecular structure.

In spite of the different coordination structures, ligand L in these compounds is in the same mode. The TTF moiety is not oxidized and all central C═C bond lengths of the TTF moiety (Table SI1, Supporting Information) are consistent with the range for neutral TTF.[14a,19] There is a strong intramolecular hydrogen bond (N−H···O) between the two ortho amido

dx.doi.org/10.1021/ic402993y | *Inorg. Chem.* 2014, 53, 3078−3087

groups, forming a stable seven-membered ring structure.[14b] More importantly, the pyridyl groups are not in the same plane of the TTF skeleton, and there is not direct conjugation between the TTF and coordination moieties; consequently, no direct intramolecular charge transfer exists.

Redox Properties of the Compounds. The redox properties of TTF derivatives have attracted much attention in evaluating their electron-donating ability as molecular electronic materials. The electrochemical properties of the ligand L and the coordination compounds **1**−**3** were investigated by cyclic voltammetry (CV) and redox spectral analysis to examine the redox potentials of the central TTF donor. Solid-state CVs were measured using the ML/ITO electrodes. As usually observed in TTF derivatives, two pairs of reversible one-electron redox waves, $E_{1/2}{}^1 = 0.553$ V and $E_{1/2}{}^2 = 0.792$ V, were observed for the ligand L (Figure 4, black line), corresponding to the $TTF^{\bullet+}/TTF$ and $TTF^{2+}/TTF^{\bullet+}$ redox couples.[7a−c] The appropriate first-step oxidation potential of the TTF moiety shows the electron donor property of ligand L. Similarly, two pairs of one-electron redox waves were observed for coordination compounds **1**−**3**. The redox potentials of them do not shift significantly in comparison with that of the ligand L, which is reasonable because the metal coordination centers do not directly conjugate with the TTF moiety. Potential shifts are usually observed for those conjugated systems of TTF−metal coordination compounds due to electron transfer through the conjugated bridge.[7b,t]

Chemical oxidations of the ligand L and complex **1** in CH_2Cl_2−CH_3CN (1:1 by volume) were carried out by successive addition of $Fe(ClO_4)_3{\cdot}6H_2O$ as oxidizing reagent[20a−d] (CAUTION: All metal perchlorates must be regarded as potentially explosive. Only a small amount of compound should be prepared, and it should be handled with caution). The changes of UV−vis absorption spectra of L were recorded in Figure 5a. The compound L has a moderately intense broad absorption band at about 455 nm (Figure 5a, black line). At first, addition of increasing amounts of $Fe(ClO_4)_3{\cdot}6H_2O$ leads to development of two intense bands at 440 and 770 nm, which shows the characteristic bands of $TTF^{\bullet+}$.[13a,20] With addition of 2.8 equiv of Fe^{3+}, the intensity of the new band reaches the maximum. Upon further addition of $Fe(ClO_4)_3{\cdot}6H_2O$, the absorption intensity at 440 and 770 nm starts to decrease and a new absorption band emerges at 660 nm that should be attributed to TTF^{2+}. The change of UV−vis absorption spectra of compound **1** is the same as that of ligand L in the same solvent (Figure 5b). The results further indicate that the TTF redox center and the metal coordination center are independent of each other in the molecules, and no direct charge transfer occurs between them. Therefore, an extra added electron acceptor is necessary to fabricate a donor−acceptor photoelectric system. The Fe ion is not coordinated with L during chemical oxidation, which is verified by EDS measurements for the oxidation products (Figure SI2, Supporting Information).

Photocurrent Response of the Microcrystal Electrodes. As the well-known electron donors and redox-active materials, TTF derivatives usually exhibit electroactivity and photoelectroactivity. However, the effects of metal coordination on the photocurrent response properties of TTF systems have not been reported to the best of our knowledge. To study the photocurrent response of the TTF-py compound and the role of metal coordination, a three-electrode photoelectrochemical cell consisting of a microcrystal sample of **1**−**3** decorated ITO electrode was constructed (a more detailed description is given in the Experimental Section). The MV^{2+} cation (1,1′-dimethyl-4,4′-bipyridinium dication) shows an efficient electron acceptor property and has been widely used in photoelectrochemical cells.[21] An aqueous solution of MVI_2 (0.1 mol·L^{-1}) was used as an auxiliary reagent for photocurrent generation. Figure 6a shows the photocurrent responses of the TTF compound L in the absence or presence of MV (denoted as L−MV), along with those of the blank test and MV itself. It is noticed that in the presence of MV, L shows observable and steady photocurrent response (ca. $I = 5$ μA), while that of the L or MV sole system was the same as the blank test. The result indicates that a donor (TTF)−acceptor (MV) system is necessary for photocurrent generation.

Figure 6b and 6c show the photocurrent responses of the coordination compound ML in the presence of the MV system (denoted as ML−MV), along with those of the L−MV, ML, and L systems. As shown in Figure 6b, the photocurrent of the CuL−MV system is about 30 μA, a six times increase in comparison with the L−MV system. Similarly, the photocurrent intensity of the MnL−MV system is about 20 μA, a four times increase in comparison with that of the L−MV system (Figure 6c). The effect of different transition metal coordination on the photocurrent intensity is illustrated in Figure 6d. The photocurrent of the NiL−MV system is about 7 μA, which shows no notable improvement in comparison with that of the L−MV system (5 μA). The effect of metal coordination on the photoresponsive property is in the order of Cu > Mn > Ni. This finding is very interesting, and the results have been verified by repetitive experiments.

Photocurrent Response of the Film Electrodes. To investigate the effects of the electrode preparation methods on the photocurrent response, electrodes of films **1**−**3** (denoted as M−L) were prepared by wet coating methods including the

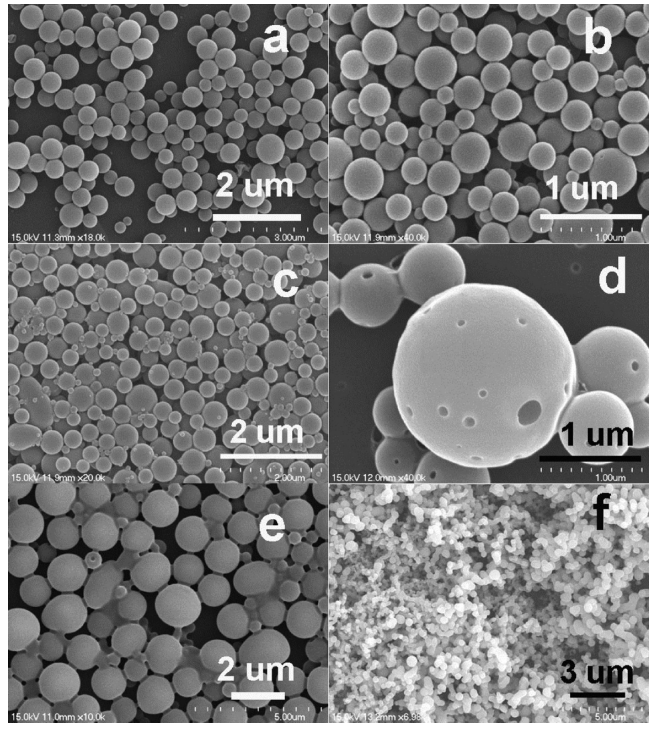

Figure 7. SEM images of the films of Ni−L (a−d) and Cu−L (e and f) prepared from different methods and solvents (room temperature). Direct solution coating method: (a) THF, (b) THF−MeOH, (e) CH_3CN−THF. Layer-by-layer reaction method: (c) $CHCl_3$−MeOH, (d) THF−THF, (f) $CHCl_3$−CH_3CN. The ratio of mixed solvent is 1:1 by volume.

dx.doi.org/10.1021/ic402993y | Inorg. Chem. 2014, 53, 3078−3087

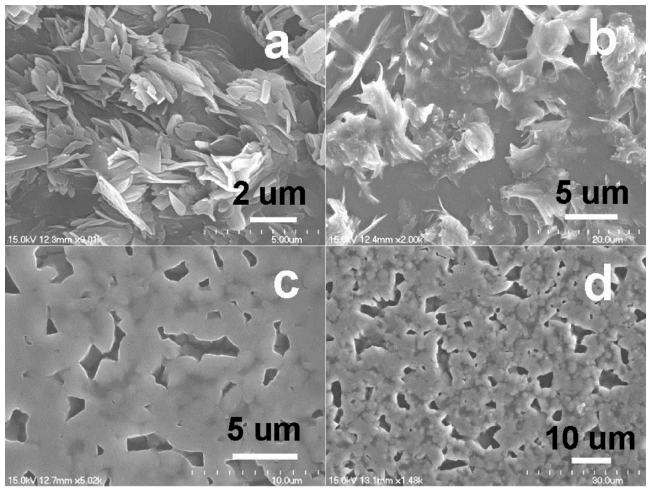

Figure 8. SEM images of the Mn−L films prepared using the layer-by-layer reaction method in different solvents (room temperature): (a) THF−THF, (b) THF−MeOH, (c) $CHCl_3$−MeOH, (d) CH_2Cl_2−MeOH. The ratio of mixed solvent is 1:1 by volume.

direct solution coating method and the layer-by-layer reaction method. FTIR spectra were used to confirm the identity of the crystals and films (Figure SI1, Supporting Information). Morphologies of the films were characterized by SEM images. Figure 7 shows the SEM images of the morphologies of Ni−L (Figure 7a−d) and Cu−L films (Figure 7e and 7f) obtained by the direct solution coating method (Figure 7a, 7b, and 7e) and layer-by-layer reaction method (Figure 7c, 7d, and 7f). The Ni−L images show that spheres about 0.3−1.0 μm diameter were obtained. The different methods and solvents used only change somewhat the size of the spheres (Figure 7a−c). In some cases there are holes on the large spheres (Figure 7d). The morphologies of Cu−L films also show spheres, similar to those of the Ni−L films. Compounds **1** and **2** are discrete small molecules and soluble to some extent in common organic solvents, which relates to their microspherical morphologies of the Cu−L and Ni−L films. As the organic solvent evaporated, the molecules quickly self-aggregated to form solvated spheres, and then with continuous release of the solvent, the hollow spheres shaped.

Figure 8 shows the SEM images of morphologies of Mn−L films. Mn−L films are completely different from those of the Ni−L and Cu−L films, showing morphologies with a lot of aggregated petaloid plates (Figure 8a and 8b), which relate to the 2-D polymeric structure of compound **3**. In dichloromethane and chloroform the aggregated plates are fused together (Figure 8c and 8d).

Photocurrent responses of the films were studied in comparison with those of the microcrystal samples (Figure 9). Some conclusions can be deduced from the repeated experimental results. (1) Photocurrent response of a carefully prepared electrode by the wet coating method is to a certain extent better than that of the electrode prepared from microcrystals both in intensity and in the shape of the peak; however, the improvement is not very remarkable. (2) The data repeatability of the wet coating films is not as good as that of the microcrystal films, and sometimes the response is poorer than the latter, because the wet method is sensitive to many factors such as the temperature, humidity, etc. (3) The morphologies of the films prepared in different solvents and the ratios of metal ion to ligand seem to have no obvious effect on the photocurrent intensity. The effect of the metal coordination on the photoresponsive property is the same as that mentioned above. Therefore, the nature of the compound itself is the main factor in influencing the photocurrent response property.

Proposed Mechanism of the Photocurrent Response. Figure 10a represents the schematic drawing of the electron transfer in the L−MV photoresponsive system. Since the potential of MV^{2+}/MV^{+} in solution is about −0.27 V (vs SEC, Figure SI3, Supporting Information) and the first oxidation potential of compound **L** is +0.55 V (TTF^{+}/TTF, vs SEC, Figure SI4, Supporting Information), no actual electron transfer exists between species TTF^{0} and MV^{2+}. When the L/ITO electrode is subjected to excitation by irradiation, the electron on the excited state of TTF is easy to be lost with the cooperation of the electron acceptor MV^{2+} and then a cathodic photocurrent is generated.

Although compounds **1**, **2**, and **3** belong to mononuclear, dinuclear, and two-dimensional polymeric structures, respectively, the photocurrent intensity seems to have no direct relationship to the structures. The fundamental molecular structures of the compounds are the same: a neutral TTF moiety with two amide−methylene−py arms which coordinate

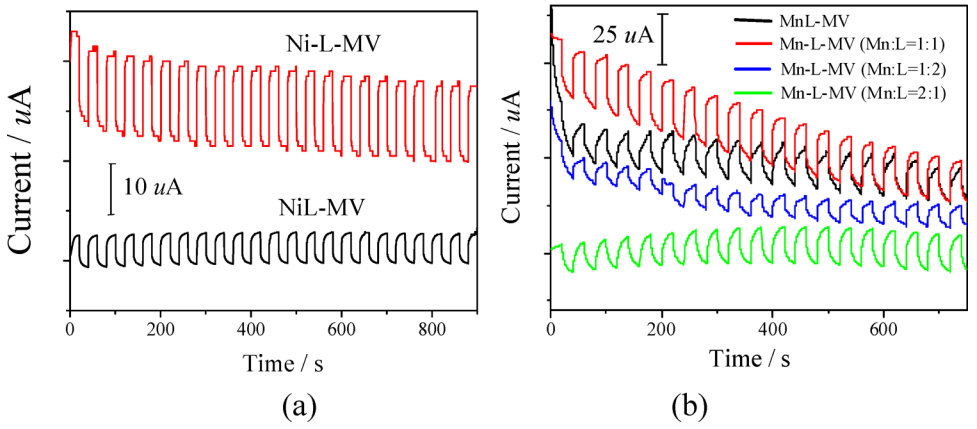

Figure 9. (a) Comparison of the photocurrent response of the film (Ni−L) modified electrodes with that of the relative compound **1** (NiL) modified electrodes upon repetitive irradiation in the presence of MV. (b) Comparison of the photocurrent response of the film (Mn−L, at different ratios of metal ion to ligand) modified electrodes with that of the relative compound **3** (MnL) modified electrodes upon repetitive irradiation in the presence of MV (three-electrode system, 0.10 mol·L^{-1} aqueous solution of Na_2SO_4). Lines are separated to be of clarity, and the *Y* axis only shows the relative current intensity.

dx.doi.org/10.1021/ic402993y | *Inorg. Chem.* 2014, 53, 3078−3087

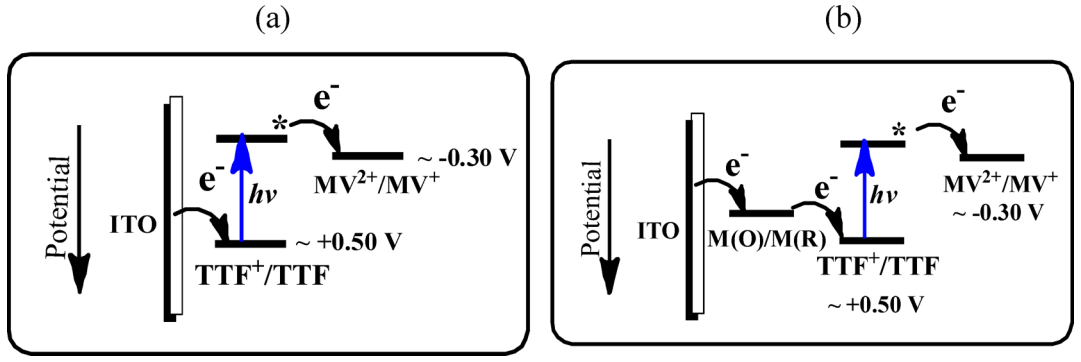

Figure 10. Schematic drawing of electron transfer in the (a) L−MV and (b) ML−MV photoresponsive systems.

to the dicationic transition metal ion by the py group. Since all electrode preparation and measurement conditions are the same, the different effect of the metal coordination centers on photoresponsive behaviors should result from the nature of the metal ion. On the basis of the knowledge of coordination chemistry, the Cu(I) and Mn(II) metals are easily oxidized to Cu(II) and Mn(III), while the Ni(II) center is a redox-inactive species that can only be oxidized to Ni(III) in a specific coordination sphere, such as macrocyclic ligands.[22] From this viewpoint, it is reasonable that the redox centers of Cu(I) and Mn(II) should play an important role in the enhancement of the photocurrent of the ML−MV systems, and it is also reasonable that the photocurrent intensity of the NiL−MV system is similar to that of the L−MV system. How do they work? A mechanism is proposed in Figure 10b. The redox-active metal coordination center might act as an electron carrier; when the TTF moiety is excited and the electron−hole separated, the neighboring metal centers transfer an electron immediately to the hole, and they subsequently obtain an electron from the electrode. This process increases the inner electron transfer in the electrode material. The cathodic photocurrent supports this mechanism. To further confirm the effect of the coordination center, noncoordinating tetra(methylthio)tetrathiafulvalene (TMTTTF) was synthesized using a modified method according to the literature.[23] Photocurrent responses of the TMTTTF-modified electrode and the electrode consisting of both TMT−TTF and Mn^{2+} ion are measured (Figure 11). The result indicates that there is no apparent effect of metal ion on the photocurrent response for a noncoordinating TTF system.

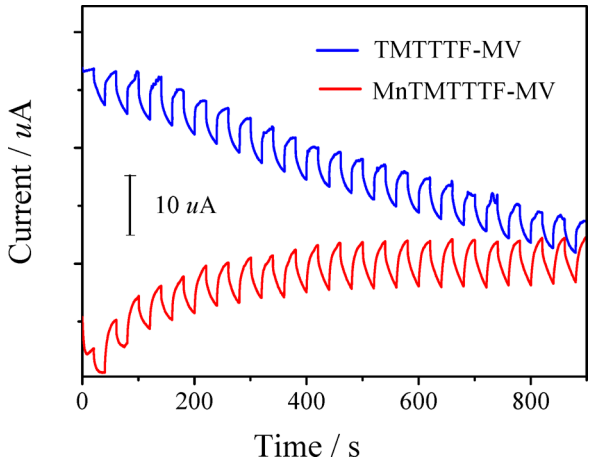

Figure 11. Comparison of the photocurrent response of the noncoordinating TMTTTF-modified electrode with that of the electrode consisting of both TMT−TTF and Mn^{2+} ion upon repetitive irradiation in the presence of MV.

CONCLUSIONS

Three TTF and divalent transition metal coordination dyads are designed and prepared, which are interesting multifunctional molecule-based materials. The spectroscopic and electrochemical properties of these complexes indicate that they are electrochemically active materials, and no direct charge transfer occurs between the TTF moiety and the metal coordination center. Photocurrent measurement shows that the TTF ligand L is an effective photoelectric conversion material in the presence of MV electron acceptor. The role of metal coordination centers in photocurrent response is examined. The redox-active metal coordination center plays an important role in the improvement of photocurrent conversion. The morphologies of the films and methods of electrode preparation and the ratios of the metal ion to ligand seem to have no obvious effect on the photocurrent response. The morphologies of M−L films and the effect of the coordination center on the photocurrent behaviors are discussed based on structural analysis. This discovery is significant in helping to design and explore new photoelectrode active materials with inorganic and organic hybrid molecular systems.

ASSOCIATED CONTENT

Supporting Information

FTIR of the ligand, M−L films prepared by the layer-by-layer coating method and the ML crystals; EDS of the ligand (a) and crystal **1** (b) after oxidation by $Fe(ClO_4)_3$; cyclic voltammogram of MVI_2 (10^{-3} mol·L^{-1}) in DMF; cyclic voltammogram of L (10^{-3} mol·L^{-1}) in CH_2Cl_2−CH_3CN (1:1 by volume); selected bond lengths (Å) of **1**−**3**; crystallographic data of **1**−**3** in CIF format. This material is available free of charge via the Internet at http://pubs.acs.org.

AUTHOR INFORMATION

Corresponding Authors

*E-mail: zhuqinyu@suda.edu.cn.
*E-mail: daijie@suda.edu.cn.

Notes

The authors declare no competing financial interest.

ACKNOWLEDGMENTS

We gratefully acknowledge financial support by the NSF of China (21171127 and 21371125), the Priority Academic Program Development of Jiangsu Higher Education Institutions,

and the Program of Innovative Research Team of Soochow University.

REFERENCES

(1) (a) Heremans, P.; Cheyns, D.; Rand, B. P. *Acc. Chem. Res.* **2009**, *42*, 1740−1747. (b) Wang, C. L.; Dong, H. L.; Hu, W. P.; Liu, Y. Q.; Zhu, D. B. *Chem. Rev.* **2012**, *112*, 2208−2267. (c) Wu, Y.; Zhu, W. *Chem. Soc. Rev.* **2013**, *42*, 2039−2058.

(2) (a) Li, Y. *Acc. Chem. Res.* **2012**, *45*, 723−733. (b) D′Souza, F.; Ito, O. *Chem. Soc. Rev.* **2012**, *41*, 86−96. (c) Dong, H.; Zhu, H.; Meng, Q.; Gong, X.; Hu, W. *Chem. Soc. Rev.* **2012**, *41*, 1754−1808. (d) Duan, C.; Zhang, K.; Zhong, C.; Huang, F.; Cao, Y. *Chem. Soc. Rev.* **2013**, *42*, 9071−9104.

(3) (a) Fujiwara, H.; Sugishima, Y.; Tsujimoto, K. *Tetrahedron Lett.* **2008**, *49*, 7200−7203. (b) Tsujimoto, K.; Ogasawara, R.; Fujiwara, H. *Tetrahedron Lett.* **2013**, *54*, 1251−1255.

(4) (a) Kakinuma, T.; Kojima, H.; Kawamoto, T.; Mori, T. *J. Mater. Chem. C* **2013**, *1*, 2900−2905. (b) Nakanishi, T.; Kojima, T.; Ohkubo, K.; Hasobe, T.; Nakayama, K.; Fukuzumi, S. *Chem. Mater.* **2008**, *20*, 7492−7500.

(5) Pfattner, R.; Pavlica, E.; Jaggi, M.; Liu, S.-X.; Decurtins, S.; Bratina, G.; Veciana, J.; Mas-Torrent, M.; Rovira, C. *J. Mater. Chem. C* **2013**, *1*, 3985−3988.

(6) (a) Nishikawa, H.; Kojima, S.; Kodama, T.; Ikemoto, I.; Suzuki, S.; Kikuchi, K.; Fujitsuka, M.; Luo, H.; Araki, Y.; Ito, O. *J. Phys. Chem. A* **2004**, *108*, 1881−1890. (b) Saha, S.; Johansson, E.; Flood, A. H.; Tseng, H.-R.; Zink, J. I.; Stoddart, J. F. *Chem.—Eur. J.* **2005**, *11*, 6846−6858.

(7) (a) Derf, F. L.; Mazari, M.; Mercier, N.; Levillain, E.; Trippé, G.; Riou, A.; Richomme, P.; Becher, J.; Garín, J.; Orduna, J.; Gallego-Planas, N.; Gorgues, A.; Sallé, M. *Chem.—Eur. J.* **2001**, *7*, 447−455. (b) Lu, H.; Xu, W.; Zhang, D.; Chen, C.; Zhu, D. *Chem. Commun.* **2005**, 4777−4779. (c) Shatruk, M.; Ray, L. *Dalton Trans.* **2010**, *39*, 11105−11121. (d) Iwahori, F.; Golhen, S.; Ouahab, L.; Carlier, R.; Sutter, J.-P. *Inorg. Chem.* **2001**, *40*, 6541−6542. (e) Canevet, D.; Sallé, M.; Zhang, G.; Zhang, D.; Zhu, D. *Chem. Commun.* **2009**, 2245−2269. (f) Madalan, A. M.; Réthoré, C.; Avarvari, N. *Inorg. Chim. Acta* **2007**, *360*, 233−240. (g) Yokota, S.; Tsujimoto, K.; Hayashi, S.; Pointillart, F.; Ouahab, L.; Fujiwara, H. *Inorg. Chem.* **2013**, *52*, 6543−6550. (h) Riobé, F.; Avarvari, N. *Chem. Commun.* **2009**, 3753−3755. (i) Réthoré, C.; Fourmigué, M.; Avarvari, N. *Chem. Commun.* **2004**, 1384−1385. (j) Pointillart, F.; Golhen, S.; Cador, O.; Ouahab, L. *Dalton Trans.* **2013**, *42*, 1949−1960. (k) Pointillart, F.; Maury, O.; Gal, Y. L.; Golhen, S.; Cador, O.; Ouahab, L. *Inorg. Chem.* **2009**, *48*, 7421−7429. (l) Keniley, L. K.; Ray, L.; Kovnir, K.; Dellinger, L. A.; Hoyt, J. M.; Shatruk, M. *Inorg. Chem.* **2010**, *49*, 1307−1309. (m) Dupont, N.; Ran, Y.-F.; Jia, H.-P.; Grilj, J.; Ding, J.; Liu, S.-X.; Decurtins, S.; Hauser, A. *Inorg. Chem.* **2011**, *50*, 3295−3303. (n) Keniley, L. K.; Dupont, N., Jr.; Ray, L.; Ding, J.; Kovnir, K.; Hoyt, J. M.; Hauser, A.; Shatruk, M. *Inorg. Chem.* **2013**, *52*, 8040−8052. (o) Nguyen, T. L. A.; Demir-Cakan, R.; Devic, T.; Morcrette, M.; Ahnfeldt, T.; Auban-Senzier, P.; Stock, N.; Goncalves, A.-M.; Filinchuk, Y.; Tarascon, J.-M.; Férey, G. *Inorg. Chem.* **2010**, *49*, 7135−7143. (p) Nguyen, T. L. A.; Devic, T.; Mialane, P.; Rivière, E.; Sonnauer, A.; Stock, N.; Demir-Cakan, R.; Morcrette, M.; Livage, C.; Marrot, J.; Tarascon, J.-M.; Férey, G. *Inorg. Chem.* **2010**, *49*, 10710−10717. (q) Liu, W.; Xiong, J.; Wang, Y.; Zhou, X.-H.; Wang, R.; Zuo, J.-L.; You, X.-Z. *Organometallics* **2009**, *28*, 755−762. (r) Xiong, J.; Liu, W.; Wang, Y.; Cui, L.; Li, Y.-Z.; Zuo, J.-L. *Organometallics* **2012**, *31*, 3938−3946. (s) Qin, Y.-R.; Zhu, Q.-Y.; Huo, L.-B.; Shi, Z.; Bian, G.-Q.; Dai, J. *Inorg. Chem.* **2010**, *49*, 7372−7381. (t) Biet, T.; Cauchy, T.; Avarvari, N. *Chem.—Eur. J.* **2012**, *18*, 16097−16103.

(8) Lorcy, D.; Bellec, N.; Fourmigué, M.; Avarvari, N. *Coord. Chem. Rev.* **2009**, *253*, 1398−1438.

(9) (a) Pointillart, F.; Bourdolle, A.; Cauchy, T.; Maury, O.; Gal, Y. L.; Golhen, S.; Cador, O.; Ouahab, L. *Inorg. Chem.* **2012**, *51*, 978−984. (b) Pointillart, F.; Cauchy, T.; Gal, Y. L.; Golhen, S.; Cador, O.; Ouahab, L. *Inorg. Chem.* **2010**, *49*, 1947−1960. (c) Setifi, F.; Ouahab, L.; Golhen, S.; Yoshida, Y.; Saito, G. *Inorg. Chem.* **2003**, *42*, 1791−1793. (d) Wang, L.; Zhang, B.; Zhang, J. *Inorg. Chem.* **2006**, *45*, 6860−6863. (e) Pointillart, F.; Gal, Y. L.; Golhen, S.; Cador, O.; Ouahab, L. *Inorg. Chem.* **2008**, *47*, 9730−9732.

(10) (a) Wu, J.; Dupont, N.; Liu, S.-X.; Neels, A.; Hauser, A.; Decurtins, S. *Chem. Asian J.* **2009**, *4*, 392−399. (b) Jia, C.; Liu, S.-X.; Tanner, C.; Leiggener, C.; Neels, A.; Sanguinet, L.; Levillain, E.; Leutwyler, S.; Hauser, A.; Decurtins, S. *Chem.—Eur. J.* **2007**, *13*, 3804−3812. (c) Jia, C.; Liu, S.-X.; Ambrus, C.; Neels, A.; Labat, G.; Decurtins, S. *Inorg. Chem.* **2006**, *45*, 3152−3154.

(11) Bivaud, S.; Balandier, J.-Y.; Chas, M.; Allain, M.; Goeb, S.; Sallé, M. *J. Am. Chem. Soc.* **2012**, *134*, 11968−11970.

(12) Wang, R.; Kang, L.-C.; Xiong, J.; Dou, X.-W.; Chen, X.-Y.; Zuo, J.-L.; You, X.-Z. *Dalton Trans.* **2011**, *40*, 919−926.

(13) (a) Zhu, Q.-Y.; Huo, L.-B.; Qin, Y.-R.; Zhang, Y.-P.; Lu, Z.-J.; Wang, J.-P.; Dai, J. *J. Phys. Chem. B* **2010**, *114*, 361−367. (b) Zhu, Q.-Y.; Liu, Y.; Lu, W.; Zhang, Y.; Bian, G.-Q.; Niu, G.-Y.; Dai, J. *Inorg. Chem.* **2007**, *46*, 10065−10070.

(14) (a) Devic, T.; Avarvari, N.; Batail, P. *Chem.—Eur. J.* **2004**, *10*, 3697−3707. (b) Baudron, S. A.; Avarvari, N.; Canadell, E.; Auban-Senzier, P.; Batail, P. *Chem.—Eur. J.* **2004**, *10*, 4498−4511.

(15) *CrystalClear*; Rigaku Corp.: 1999. *CrystalClear Software User's Guide*; Molecular Structure Corp.: 2000. Pflugrath, J. W. *Acta Crystallogr., Sect. D* **1999**, *55*, 1718−1725.

(16) Sheldrick, G. M. *SHELXS-97, Program for structure solution*; Universität of Göttingen: Göttingen, Germany, 1999. Sheldrick, G. M. *SHELXL-97, Program for structure refinement*; Universität of Göttingen: Göttingen, Germany, 1997.

(17) (a) Chong, J. H.; Maclachian, M. J. *J. Org. Chem.* **2007**, *72*, 8683−8690. (b) Oshio, H.; Watanabe, T.; Ohto, A.; Ito, T.; Masuda, H. *Inorg. Chem.* **1996**, *35*, 472−479. (c) Xie, Y. B.; Ma, Z. C.; Wang, D. *J. Mol. Struct.* **2006**, *784*, 93−97. (d) Zhang, D. Q.; Ding, L.; Xu, W.; Jin, X. L.; Zhu, D. B. *Chem. Lett.* **2001**, 242−243.

(18) Healy, P. C.; Pakawatchai, C.; White, A. H. *J. Chem. Soc., Dalton Trans.* **1983**, 1917−1927.

(19) Bouguessa, S.; Gouasmia, A. K.; Golhen, S.; Ouahab, L.; Fabre, J. M. *Tetrahedron Lett.* **2003**, *44*, 9275−9278.

(20) (a) Asakawa, M.; Ashton, P. R.; Balzani, V.; Credi, A.; Hamers, C.; Mattersteig, G.; Montalti, M.; Shipway, A. N.; Spencer, N.; Stoddart, J. F.; Tolley, M. S.; Venturi, M.; White, A. J. P.; Williams, D. J. *Angew. Chem., Int. Ed. Engl.* **1998**, *37*, 333−337. (b) Balzani, V.; Credi, A.; Mattersteig, G.; Matthews, O. A.; Raymo, F. M.; Stoddart, J. F.; Venturi, M.; White, A. J. P.; Williams, D. J. *J. Org. Chem.* **2000**, *65*, 1924−1936. (c) Asakawa, M.; Higuchi, M.; Mattersteig, G.; Nakamura, T.; Pease, A. R.; Raymo, F. M.; Shimizu, T.; Stoddart, J. F. *Adv. Mater.* **2000**, *12*, 1099−1102. (d) Tseng, H.-R.; Vignon, S. A.; Celestre, P. C.; Perkins, J.; Jeppesen, J. O.; Fabio, A. D.; Ballardini, R.; Gandolfi, M. T.; Venturi, M.; Balzani, V.; Stoddart, J. F. *Chem.—Eur. J.* **2004**, *10*, 155−172. (e) Ashton, P. R.; Balzani, V.; Becher, J.; Credi, A.; Fyfe, M. C. T.; Mattersteig, G.; Menzer, S.; Nielsen, M. B.; Raymo, F. M.; Stoddart, J. F.; Venturi, M.; Williams, D. J. *J. Am. Chem. Soc.* **1999**, *121*, 3951−3957.

(21) (a) Yasutomi, S.; Morita, T.; Kimura, S. *J. Am. Chem. Soc.* **2005**, *127*, 14564−14565. (b) Driscoll, P. F.; Douglass, E. F.; Phewluangdee, M., Jr.; Soto, E. R.; Cooper, C. G. F.; MacDonald, J. C.; Lambert, C. R.; McGimpsey, W. G. *Langmuir* **2008**, *24*, 5140−5145. (c) Matsuoka, K.; Akiyama, T.; Yamada, S. *J. Phys. Chem. C* **2008**, *112*, 7015−7020. (d) Trammell, S. A.; Dressick, W. J.; Melde, B. J.; Moore, M. *J. Phys. Chem. C* **2011**, *115*, 13446−13461. (e) Zhu, M.; Dong, Y.; Xiao, B.; Du, Y.; Yang, P.; Wang, X. *J. Mater. Chem.* **2012**, *22*, 23773−23779.

(22) Bhattacharya, S.; Saha, B.; Dutta, A.; Banerjee, P. *Coord. Chem. Rev.* **1998**, *170*, 47−74 and references therein..

(23) Wu, P.; Saito, G.; Imaeda, K.; Shi, Z.; Mori, T.; Enoki, T.; Inokuchi, H. *Chem. Lett.* **1986**, 441−444.